Static Analysis of Nippers Pinch

Gregorij Kurillo, BSc ▪ Tadej Bajd, DSc ▪ Roman Kamnik, DSc

Faculty of Electrical Engineering, University of Ljubljana, Ljubljana, Slovenia

■ **ABSTRACT**

The purpose of the study was to present a method for the assessment of finger joint torques in two-fingered precision grips. The static analysis of various grips is important for the analysis of the mechanics of a human hand and the functional evaluation of grasping. We have built a grip-measuring device assessing the endpoint forces of two-oppositional grips. Through the simultaneous use of an optical measuring system and the grip-measuring device, the finger positions and the grip force acting on the object were obtained. A recursive computational method was used within the proposed static model of the finger to calculate the finger joint torques. In the paper a three-dimensional static model of the grip is presented and the calculated finger joint torques are shown. The repeatability within subject is analyzed for the assessed grip force and finger joint torques. The estimated joint torques corresponds to the amount of load on the finger joints during the isometric muscle contraction in nippers pinch. ■

KEY WORDS: biomechanics, finger, grip force, precision grip.

INTRODUCTION

The loss of hand functionality from a central nervous system (CNS) injury or a hand injury can greatly influence a person's everyday life (1–3). Different methods of rehabilitation and therapy, including functional electrical stimulation (FES), can help such people regain a certain degree of functionality in their hands (2,3). The analysis of the mechanical properties of the fingers and assessment of forces and torques acting on the finger joints can provide additional information about hand mobility (4,5) and the amount of load on the fingers during daily activities (6–8).

Address correspondence and reprint requests to: Gregorij Kurillo, Faculty of Electrical Engineering, University of Ljubljana, Trzaska 25, 1000 Ljubljana, Slovenia, Email: gregorijk@robo.fe.uni-lj.si.

Neuromodulation, Volume 6, Number 3, 2003 166–175

Grip-force assessment is also an important factor in hand functionality evaluation (1,9,10). In rehabilitation therapy, most measurements are made by various types of dynamometers, which measure only strength and thus provide only partial information on a subject's grip (11). Capturing the grip force vector (grip strength and direction of the force) can give additional knowledge on the grip performance and coordination (2,4,9). Different researchers (6–8) have proposed instrumented objects to assess the force vectors acting on objects that are in shape and size similar to the objects used in daily living. Instrumented objects allow real-time measurements of the force during the observed grip. In this paper we propose a grip-measuring device with a commercial force sensor to measure grip forces in two-fingered grips.

The assessment of the finger joint torques and fingertip forces provides more information on the mechanics of the fingers and describes the amount of load on the finger joints during a grip applied (5). Different researchers (4,5,12,13) have presented models for the assessment of joint torques from the measured or simulated fingertip force. The purpose of our study was to investigate a method for the static analysis of two-fingered grips that employs simultaneous measurement of the fingertip force and finger joint positions, providing thus the necessary information for the calculation of the joint torques.

In this research the static force analysis of a two-fingered precision grip was performed. A grip-measuring device was designed to record the force vector acting on the measuring object in two-oppositional grips (14,15). Assessing the magnitude and direction of the fingertip force vector can provide an insight into the subject's grip force control which is important when applying motion to the object or keeping the object in a secure grip (9). In case of a neurologic condition or trauma, such information may be useful to determine deviations of one's grasp compared to a healthy subject. The ability to produce strong and well-coordinated two-fingered grip can be reduced due to a brain or spinal cord injury, damage to the ulnar or median nerves, or arthritis (9). The grip force analysis can provide additional information that can be used in hand diagnosis and treatment, for the selection of FES patterns of the upper extremities, and for the functional evaluation of the hand after a reconstructive surgery (2,9,12).

Our study is focused on a nippers pinch that is characterized as a precision grip (14,16). The object is grasped between the finger pads of the thumb and index finger, providing good sensory feedback on the properties of the object. The two fingers in nippers pinch are extended, which allows higher forces to be exerted. The grip is aimed to grasp and manipulate small objects (eg, a pencil, paper clip) where a fine force control and good stability of the object is required. Two-fingered precision grips are used in many activities of daily living (eg, picking up small objects, turning a knob, writing with a pen) and are therefore a significant goal for the restoration of the hand function (4,12), particularly after a hand injury or stroke.

To assess the finger joint torques during a grip, the measurements of the fingertip force and the posture of the fingers are needed. The finger positions were obtained by the optical measuring system. The hand and the finger joints were marked with markers to capture their relative position to the object. It has been demonstrated that optical measurements can be used successfully for the assessment of finger joint positions (17–19). The validity of the method has been addressed by Rash and colleagues (17) who compared the optical 3-D motion analysis with a 2-D video fluoroscopic recording of a finger motion. They reported that the accuracy of such a method of marker placement for the measurement of joint angles is comparable to the errors found in clinical goniometry (± 5°).

In our experiment the grip force was measured by the grip-measuring device developed. From the obtained results, the finger joint torques were calculated recursively (20) by the use of the proposed static model of the human finger. Some results of the measured grip force and joint torques are presented in the paper to provide an insight into the proposed assessment method.

METHODS

Model

In our investigation each finger was modeled as a serial manipulator attached to the palm. The three phalanxes of the finger were modeled as rigid segments connected with different types of joints (2). We used four degrees of freedom (DOF) to describe the movement of each finger (Fig. 1). The proposed complexity of the model is sufficient for the analysis of a simple finger movement (4). Universal joint (2 DOF) models the flexion-extension and adduction-abduction of the proximal joint. Two rotational joints (1 DOF) are used to model the flexion-extension of the middle and distal joints. The approximate mass of the segments for an average male human hand was considered in the calculations. The data were obtained from the Institute of Anatomy, Medical Faculty, University of Ljubljana. The center of mass for each segment was determined by an approximation of the phalanx with a cone-shaped homogenous rigid body (13), where the diameters of the knuckles were measured before the experiment.

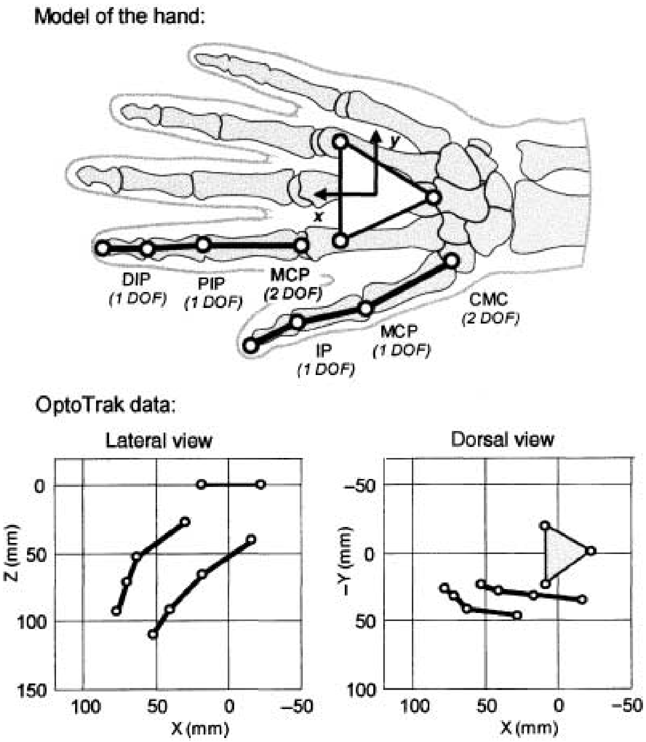

Figure 1. Each finger of the proposed model of the hand has four degrees of freedom (above). A three-dimensional model of the precision grip was assessed with the OptoTrak system (below).

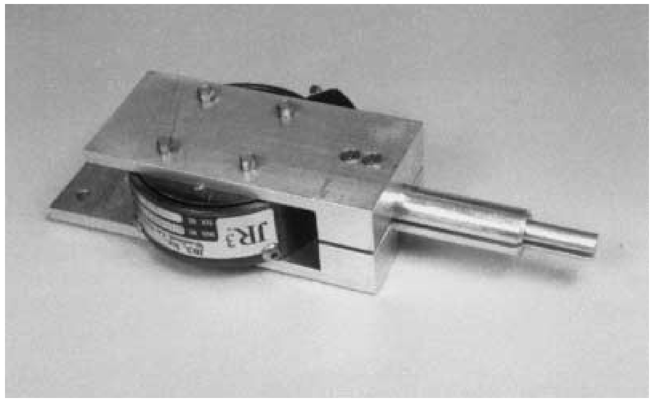

Figure 2. Grip-measuring device was designed to measure the endpoint forces of two-oppositional grips. The instrument is based on the robotic force-wrist sensor and designed to suit a human grip. The two metal parts, which shape into a circular stick to fit human fingers, allow the transmission of fingertip force to the sensory unit.

Method Overview

To calculate the finger joint torques, the measurements of the fingertip force and position of the fingers, relatively to the object, were needed (20). Hand posture was assessed by the optical measuring system OptoTrak (Northern Digital, Inc., Waterloo, Canada) which can accurately (with the accuracy of 0.1 mm) measure the three-dimensional position of infrared markers placed in front of the system of three cameras. Forces acting on the object were measured simultaneously through a specially designed grip-measuring device (Fig. 2).

The OptoTrak system consists of three cameras with fixed relative position and orientation. The active infrared markers are placed in front of the optical system and have to be visible during the measurement. The exact three-dimensional coordinates of each marker are calculated by the system from the known geometry and expressed in the world coordinate system (20), which is the coordinate system defined by the calibration procedure. The system must be calibrated before each measurement session by the calibration plate placed in front of the cameras. Two sets of OptoTrak cameras situated in the opposing direction were used in our experiment. For convenience, all data measured were transformed into a local coordinate system of the sensor (SCS), defined by the three markers applied on the top surface of the grip-measuring device. The defined coordinate system matched with the internal coordinate system of the force sensor. We also defined a hand coordinate system (HCS) on the dorsal side of the hand to follow the relative position of the hand to the grip-measuring device. Two markers were applied at the distal ends of the second and fourth metacarpal and the third marker was attached at the proximal end of the third metacarpal bone (Fig. 1). All three markers formed a triangle on a dorsal plane that was used to position the coordinate system of the hand. The x-axis was oriented along the third metacarpal bone, the z-axis was defined by the normal of the dorsal triangle and oriented into the palm of the hand and the y-axis was parallel to the flexion-extension axis of the metacarpo-phalangeal joint (17).

The rest of markers were attached to the lateral side of the thumb and index finger to mark the position of the joint axes and fingertip. The center of rotation for each joint was determined from the visible anatomic landmarks (15,17). The proximal interphalangeal (PIP) and distal interphalangeal (DIP) joint locations were determined from the

PIP and DIP joint lines on the palmar side of each finger and the metacarpo-phalangeal (MCP) joint location was approximated from the location of the palmar crease at the end of the second metacarpal (17). The markers were placed laterally into the approximated centers of rotation. The placement of the markers was inspected visually and by the optical system where the subject's finger movement was recorded to see whether the relative distance between each two subsequent joints changed. The corrections of the marker positions were made accordingly.

From the measured marker locations, the centers of joints were determined (Fig. 1) and local coordinate systems were placed into the hand segments using the notation adopted from the analysis of mechanical manipulators (20). The joint coordinate system of the segment *i* (JCSi) was placed at the distal end of the corresponding segment as shown in Figure 4. The origin of the coordinate system was translated in the direction perpendicular to the sagittal plane to the center of the knuckle. The *z*-axis of the finger coordinate system corresponded to the normal vector of the sagittal plane defined by the three markers located on the lateral side of the finger. The *x*-axis of each joint coordinate system was defined in the direction of the phalanx obtained from the location of two subsequent markers. The *y*-axis vector was then determined to obtain an orthogonal coordinate system.

A grip-measuring device (Fig. 2) was designed to measure the endpoint forces of two-oppositional grips. The instrument is based on the robotic force-wrist sensor JR3 (JR3, Inc., Woodland, CA) that measures forces in three directions of its coordinate system and a torque around the *z*-axis. The force measurement range of the sensor is 110 N in the *x* and *y* directions (horizontal plane of the sensor) and 220 N in the *z*-axis of the sensor coordinate system. The torque range of the sensor is 10 Nm. The measured force vector corresponds to the amount and direction of the tension between the upper and lower parts of the external surfaces of the sensor body. No displacement is produced due to a high rigidity of the device. The sensor consists of foil strain gauges arranged in wheatstone bridges that are connected to an external amplifier. Each of the four output channels corresponds to one force (torque) component and the cross talk between the channels is compensated. The analog outputs are sampled through an A/D unit and a producer-adjusted calibration matrix is used to transform voltages into the corresponding force (torque) components. The sensor is calibrated with respect to the internal coordinate system that is located in the center of the sensor body. The nonlinearity of the sensor is less than 1% across the range and the resolution of the measurement is 0.01 N.

The grip-measuring device developed consists of two metal parts that are shaped in the form of the letter "L" with two semicircular sticks attached to the front side of the device where the two "L" parts come close together (Fig. 2). The space between the two parts of the measuring object prevents the two halves of the stick to contact each other, even at forces as high as 70 N. The construction allows a simple exchange of differently shaped endpoint objects. When a person grasps the measuring stick, the grip force is translated to the sensor yielding the information on the grip force vector. The metal construction has some compliance in the vertical plane at high-level forces due to the elasticity of the metal and relatively large moment arm (14 cm); therefore the measured force would differ (for about 4% at 35 N) from the applied force at the endpoint of the measuring object. The effect of the compliance on the other two force components in the horizontal plane of the device is not critical because the rigidity of the metal frame is much higher in these two directions. The influence of the moment arm from the point of contact to the sensor coordinate system was compensated through a recalibration procedure. Different weights were placed at the center of the sensor and at the distal end of the device and the measured forces were compared. The calibration matrix was corrected accordingly. The results show (Fig. 3) that the metal frame attached to the sensor does not influence the linearity and accuracy of the measurements after the modification of the calibration matrix. The force characteristic of the measurement at the endpoint object of the grip-measuring device (Fig. 3) is linear with the error of 1.4%. During the experiment we assume that the subject grasps the measuring stick at the distal part of the device.

In the experiment the force vector components measured by the grip-measuring device were

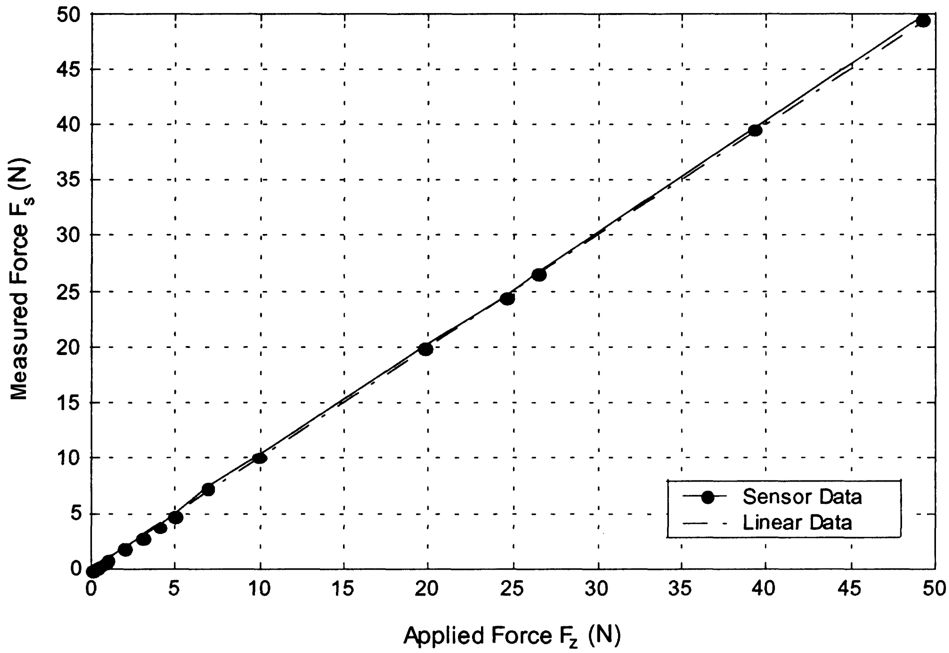

Figure 3. The measured output of the grip-measuring device after re-calibration of the sensor to the application of force F_z at the measuring object shows a linear dependency (error 1.4%). The solid line represents the measured force F_s in the *z*-axis of the sensor and the dotted line represents the ideal characteristic ($F_s = F_z$).

transformed into analog voltage values and sampled at the frequency of 100 Hz through the A/D unit of the OptoTrak system to obtain the simultaneous data of the grip force and positions of the finger joints. The analysis of the results and the calculation of the joint torques were performed off-line with Matlab software (The MathWorks, Inc., Natick, MA).

Analysis

We used a recursive computational method (20) to calculate the forces and torques acting between the segments of each finger. In the presented calculation the forces and torques are analyzed in the direction from the contact point to the palm of the hand, considering the finger as a serial manipulator (Fig. 4). Each of the two fingers is analyzed separately. The palm was considered as the segment #0, the proximal segment was denoted with the index #1, the middle with #2, and the distal segment with #3. The measured endpoint force and position of the fingertip marker defined the contact with the object. In the calculations we modeled the contact with the object as a point contact with friction (20). The presented model of the hand (Fig. 1) was used in the following calculations where every finger k was analyzed separately ($k = 1$ for the thumb and $k = 2$ for the index finger). All the vectors used in the equations (Eqs. 1–2) are expressed in the coordinate system of the sensor.

First, the equilibrium equations for forces are written for each segment i:

$$^{k}f_{i-1,i} - {}^{k}f_{i,i+1} + {}^{k}m_i g = 0 \qquad \text{(Eq. 1)}$$

The forces that act on the segment i of the finger k (Fig. 4) are: the gravity force $^{k}m_i{\cdot}g$ (where $^{k}m_i$ is the mass of the segment and g is gravity acceleration), the force $^{k}f_{i-1,i}$ describing the force of the segment $i-1$ acting on the segment i and the negative force $^{k}f_{i,i+1}$ defining the action of the segment $i+1$ on the segment i.

Next, the equilibrium equation for the torques acting on the segment i (Fig. 4) is written with regard to the center of the corresponding finger joint:

$$^{k}T_{i-1,i} - {}^{k}T_{i,i+1} + {}^{k}r_{gi} \times {}^{k}m_i g - {}^{k}r_{fi} \times {}^{k}f_{i-1,i} = 0 \qquad \text{(Eq. 2)}$$

In Equation 2 the vector $^{k}r_{gi}$ connects the joint center with the center of mass for the segment i and $^{k}r_{fi}$ connects the joint center with the end of

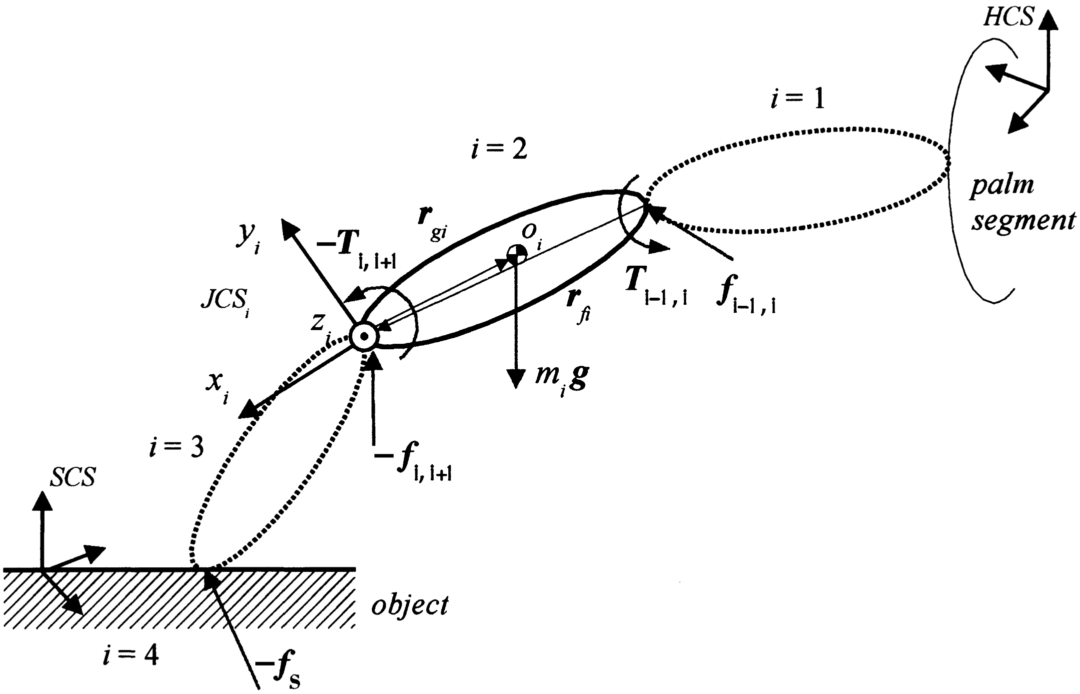

Figure 4. The static analysis of the finger model in the contact with the object. The forces and torques acting on the *i*-th segment are presented. The torques were calculated from the assessed finger joint positions and the measured endpoint force (f_s) using a recursive computational method.

the segment *i*. The torque vector ${}^kT_{i-1,i}$ describes the torque of the previous segment onto the segment *i*. ${}^kT_{i,i+1}$ is the torque vector of the next segment acting on the segment *i*. The vector product ${}^kr_{gi} \times {}^km_ig$ describes the effect of gravity force and ${}^kr_{fi} \times {}^kf_{i-1,i}$ represents the torque caused by the force ${}^kf_{i-1,i}$ acting around the origin with the moment arm ${}^kr_{fi}$ (Fig. 4). The distance vectors used were calculated from the locations of the markers, expressed in the sensor coordinate system.

Next, the force ${}^kf_{i-1,i}$ and the torque ${}^kT_{i-1,i}$ are derived from the above equations. In the first step of the recursive computation (i = 3), the negative force ${}^kf_{i,i+1}$ equals the grip force f_s measured with the force sensor and ${}^kT_{i,i+1}$ equals zero since the fingertip is not attached to the object surface (Fig. 4):

$$\begin{aligned} {}^kf_{3,4} &= -f_s \\ {}^kT_{3,4} &= 0 \end{aligned} \qquad \text{(Eq. 3)}$$

The force and torque vectors of the distal joint (i = 2) are calculated from the fingertip force:

$$\begin{aligned} {}^kf_{2,3} &= {}^kf_{3,4} - {}^km_3g \\ {}^kT_{2,3} &= -{}^kr_{g3} \times {}^km_3g + {}^kr_{f3} \times {}^kf_{3,4} \end{aligned} \qquad \text{(Eq. 4)}$$

Next, the force and torque vectors of the medial joint (i = 1) are calculated:

$$\begin{aligned} {}^kf_{1,2} &= {}^kf_{2,3} - {}^km_2g \\ {}^kT_{1,2} &= {}^kT_{2,3} - {}^kr_{g2} \times {}^km_2g + {}^kr_{f2} \times {}^kf_{1,2} \end{aligned} \qquad \text{(Eq. 5)}$$

Finally, the force and the torque acting on the proximal joint (i = 0) are determined:

$$\begin{aligned} {}^kf_{0,1} &= {}^kf_{1,2} - {}^km_1g \\ {}^kT_{0,1} &= {}^kT_{1,2} - {}^kr_{g1} \times {}^km_1g + {}^kr_{f1} \times {}^kf_{0,1} \end{aligned} \qquad \text{(Eq. 6)}$$

The same calculations (Eqs. 3–6) are repeated for the opposite finger (k = 2) while considering the end point force vector to be oriented in the opposite direction. The calculated force and torque vectors are expressed in the sensor coordinate system. In order to obtain the torques acting in the center of each joint, we must transform the calculated vectors to the corresponding joint coordinate systems using homogenous transformations (20) defined with the placement of the joint coordinate systems.

Experiments

A right-handed healthy male individual performed the precision grip nipper pinch. The subject's

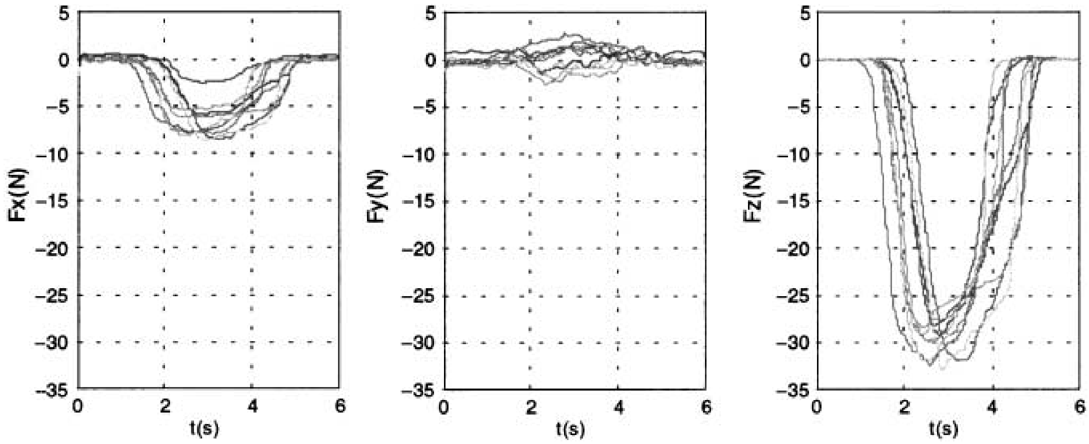

Figure 5. The force components of the grip force vector in nippers pinch as assessed in a healthy subject. The maximal force component which is perpendicular to the surface normal has a bell-shaped profile with the mean value of 30.4 ± 1.6 N within trials. The magnitudes of the other two components of the grip force vector are considerably lower. The repeatability of the results is high in *z*- and *x*-direction but low in the *y*-direction.

hand was equipped with 11 infrared markers as described in the previous section. During the experiment the grip-measuring device was attached at the edge of the table and the subject was seated on a chair located in front of the OptoTrak cameras. Two sets of cameras situated in the opposing direction were used to capture the position of all markers. The subject's forearm rested on a support with a 90° flexion of the elbow and a neutral position of the shoulder (10). The support of the forearm prevented unwanted disturbances on the grip force measurement (eg, subject's leaning onto the device). The subject was instructed to perform the precision grip on the measuring stick with low (under 20 N), medium (20–40 N), and high level force (above 40 N), keeping it steady for a moment and then slowly releasing the grip. The whole session lasted approximately 6 s. Subject had no visual feedback of the grip performed. In some cases the OptoTrak data were missing or the applied force was too low or too high with respect to the instructed force range. After the subject adjusted to the experiment procedure, 10 consecutive trials of the medium grip force were recorded and are analyzed in the paper.

RESULTS

The measured OptoTrak data of the observed grip are presented in Fig. 1 as a three-dimensional model in lateral and dorsal view of the hand coordinate system. The wire frame image reflects the posture of the hand and the position of the finger joints that are used in the recursive calculation.

The assessed grip forces during the 10 trials performed are presented in Figure 5. The grip forces shown have bell-shaped profiles along the *z*-axis of the sensor coordinate system, reaching the maximal value around 30 N. The magnitudes of the other two components of the grip force vector are considerably lower. The tangential force in the *x*-direction is negative and also reflects a bell-shaped profile. The correlation between the shapes of the two forces is very high in all trials (the average correlation coefficient c_f between the measured signals is 0.98). The force control acts mainly in the perpendicular direction to the finger pads. The results indicate that the pinch force vector is slightly rotated from normal at the point of contact to the negative *x*-axis along the tangent of the surface. This is most likely caused by the oppositional role of the thumb. In the opposition between the index finger and thumb, the two finger pads are not coplanar; therefore the thumb produces also a tangential force component to the object surface. Comparing the results of all trials (Fig. 5, Table 1) shows a significant correlation ($p < 0.01$, Pearson Correlation Coefficient is 0.791) between the peak values of the F_z and F_x force components, indicating a good repeatability of the measured pinch force. The remaining force component F_y shows more arbitrary profile. There

Table 1. The Peak Values of the Measured Grip Forces and the Corresponding Finger Joint Torques as Assessed in 10 Consecutive Trials in One Subject[a]

	Applied grip force (N)			Joint torques of thumb (Nm)				Joint torques of index finger (Nm)			
Trial	F_x	F_y	F_z	$^1T_{1y}$	$^1T_{1z}$	$^1T_{2z}$	$^1T_{3z}$	$^2T_{1y}$	$^2T_{1z}$	$^2T_{2z}$	$^2T_{3z}$
1	–5.9	–1.2	–29.0	–0.66	3.31	1.73	0.79	–0.04	2.30	0.95	0.38
2	–2.5	–0.5	–28.2	–0.26	3.15	1.27	0.59	–0.22	2.28	1.07	0.46
3	–8.5	–1.1	–32.1	–0.92	3.57	1.94	0.91	–0.00	2.63	1.21	0.54
4	–7.7	0.6	–31.7	–0.83	3.53	1.85	0.87	–0.05	2.62	1.22	0.55
5	–7.9	0.5	–29.8	–0.49	3.47	1.84	0.86	–0.19	2.58	1.13	0.51
6	–6.2	–0.8	–28.8	–0.46	3.27	1.67	0.79	–0.16	2.49	1.12	0.51
7	–5.5	2.4	–29.4	–0.28	3.47	1.63	0.73	–0.23	2.47	1.02	0.46
8	–8.2	–1.9	–32.3	–0.47	3.84	1.85	0.84	–0.20	2.74	1.15	0.52
9	–8.6	–1.6	–32.4	–0.58	3.78	1.83	0.85	–0.17	2.79	1.19	0.54
10	–7.7	0.4	–29.5	–1.00	3.31	1.71	0.79	–0.14	2.41	1.05	0.48
Mean	**–6.9**	**–0.31**	**–30.4**	**–0.56**	**3.47**	**1.73**	**0.80**	**–0.14**	**2.53**	**1.11**	**0.50**
SD	(1.9)	(1.3)	(1.6)	(0.26)	(0.22)	(0.19)	(0.09)	(0.08)	(0.17)	(0.09)	(0.06)

[a] The maximal values of the grip force components F_x and F_z have low standard deviation (SD) showing that the direction of the grip remains similar between the trials. The values of the finger joint torques indicate that the total load in the proximal joint of the thumb is considerably higher than in the joint of the index finger

is no significant correlation between F_y and F_z force components ($p > 0.05$).

The recursive computation was used with the assessed grip force and finger joint positions to obtain the joint torques (Fig. 6). The four torques, which apply to the described static model, were calculated for each finger: the torque ($^kT_{1y}$) around the adduction-abduction axis of the proximal joint and the three torques ($^kT_{1z}$, $^kT_{2z}$, $^kT_{3z}$) around the flexion-extension axes. The joint torques assessed in the thumb correspond to the carpo-metacarpal (CMC), metacarpo-phalangeal (MCP), and interphalangeal (IP) joints. The torques for the index finger describe the load in the metacarpo-phalangeal (MCP), proximal interphalangeal (PIP), and distal interphalangeal (DIP) joints.

The peak values of the measured grip force and corresponding finger joint torques obtained in each trial are gathered in Table 1. The subject was able to produce similar grip force levels in all trials where the average force in z-direction was 30.4 ± 1.6 N. Comparing the peak torque values (Table 1) indicates that the total load in the proximal joint of the thumb is considerably higher than in the joint of the index finger ($p < 0.01$, paired-samples t-test). The load in the abduction-adduction axis of the index finger in the observed precision grip is lower than for the thumb. The deviations of the assessed abduction-adduction torques in the proximal joints are high which indicates that the placement of the proximal coordinate system of a finger is more sensitive to errors.

DISCUSSION AND CONCLUSION

The purpose of this study was to present a method for the static analysis of a two-fingered precision grip. The OptoTrak system was used to capture the hand posture along with the grip-measuring device aimed to simultaneously measure the grip forces. A three-dimensional model of the hand was obtained from the measurements, showing that the optical measuring system can be helpful in the analysis of hand posture. The optical method of assessing the finger positions allows unrestrained movement and grasping of objects, providing the necessary parameters for the static analysis of the grip. The accuracy of the method depends on the accuracy of the placement of the markers onto the fingers to mark the centers of joints. The finger joint positions were assessed from the joint lines on the palmar side of the hand and corrected based on the observed flexion-extension of the finger. The assessment of the proximal joint position was found to be more sensitive to errors.

The finger joint torques were calculated from the assessed finger positions and grip force utilizing the recursive calculation method. The presented joint torques describe the amount of load

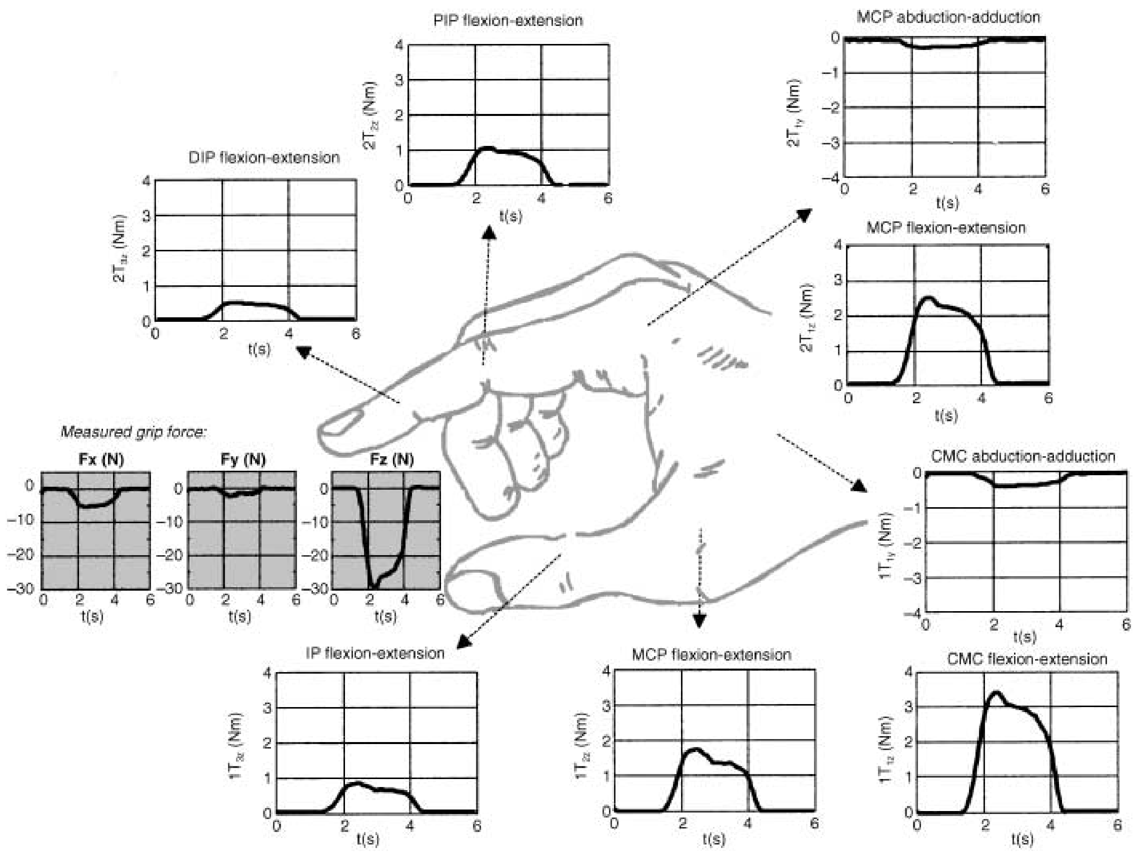

Figure 6. The measured grip force in nippers pinch and the calculated finger joint torques. The grip force has a bell-shaped profile with the peak value in the perpendicular direction to the measuring object. The torque values indicate the load on the finger joints during the observed grip.

on the joints during the grip applied. In this paper a set of 10 trials for one subject is presented. Analysis of subject-to-subject variations will be included in our future investigations.

During the experiment the subject relied on his proprioceptive feedback and had no visual information on the performance of the grip. This resulted in some diverse results in the grip force levels and duration of the grips before the subject became accustomed to the experiment procedure. Adding some additional feedback information (eg, on the duration of the trial and/or the force level reached) could improve the repeatability of the measurements and allow increased correlation of data in experiments with more subjects, who could more easily apply force levels required by the examiner. The grip-measuring device also could be used as an input device for an isometric tracking task (21) where the subject would be presented with a graphic display of the target signal and the measured grip force response. The assessment of isometric grip forces by the grip-measuring device and visual feedback from the computer screen could offer useful results for the analysis of sensory-motor control of the grip force in different grip configurations (21).

The proposed method is similar to the part of the Fugl-Meyer hand evaluation test (1) used in hemiplegic patients where the subject is asked to perform a precision grip of a pencil. With a modification of the grip-measuring device, grasps of different objects could be simulated. Differently shaped endpoint objects (eg, in the shape of a disk, sphere, cylinder, etc.) could replace the measuring stick in order to determine the forces that act on such objects in different hand postures. Such a method can be used in connection with different rehabilitation therapies, including functional electrical stimulation (FES) (2,3), to follow the improvement of a patient's condition or to train the subject in grip force control. The knowledge of forces acting on differently shaped objects is also important in ergonomics where different products and tools need to be adjusted to the human grip to minimize discomfort and injury (16).

ACKNOWLEDGMENT

The authors wish to thank Prof. Dr. Dean Ravnik, Institute of Anatomy, Medical Faculty, University of Ljubljana, for the anthropometric data of the human hand.

REFERENCES

1. Fugl-Meyer AR, Jääskö L, Leyman I, Olsson S, Steglind S. The post-stroke hemiplegic patient. A method for evaluation of physical performance. *Scand J Rehabil Med* 1975;7:13-31.
2. Towles J, Murray W, Valero-Cuevas F, Zajac F. Influence of flexor pollicis longus muscle's joint moments on the direction and magnitude of its thumb-tip force. *Proceedings of the VI IFESS*: Cleveland, OH. 2001: 291-293.
3. Peckham PH, Keith MW, Kilgore KL. Restoration of upper extremity function in tetraplegia. *Top Spinal Cord Inj Rehabil* 1999;5:33-43.
4. Valero-Cuevas FJ. Applying principles of robotics to understand the biomechanics, neuoromuscular control and clinical rehabilitation of human digits. *Proceedings of the 2000 IEEE ICRA*. San Francisco, CA. 2000: 270-275.
5. Amirouche F, Gonzalez M, Koldoff J, Tioco J, Ham K. A biomechanical study of the finger pulley system during repair. *Technol Health Care* 2002;10:23-31.
6. Memberg WD, Crago PE. Instrumented objects for quantitative evaluation of hand grasp. *J Rehab Res Dev* 1997;34:82-90.
7. Fowler NK, Nicol AC. A force transducer to measure individual finger loads during activities of daily living. *J Biomech* 1999;32:721-725.
8. Chadwick EKJ, Nicol AC. A novel force transducer for the measurement of grip force. *J Biomech* 2001;34:125-128.
9. Johanson ME, Valero-Cuevas FJ, Hentz VR. Activation patterns of the thumb muscles during stable and unstable pinch tasks. *J Hand Surg* 2001;26A:698-705.
10. Smidt GL, Rogers MR. Factors contributing to the regulation and clinical assessment of muscular strength. *Phys Ther* 1982;62:1283-1290.
11. Innes E. Handgrip strength testing. A review of the literature. *Aust Occup Ther J* 1999;46:120-140.
12. Valero-Cuevas FJ, Towles JD, Hentz VR. Quantification of fingertip force reduction in the forefinger following simulated paralysis of extensor and intrinsic muscles. *J Biomech* 2000;33:1601-1609.
13. Sancho-Bru JL, Pérez-González A, Vergara-Monedero M, Giurintano D. A 3-D dynamic model of human finger for studying free movements. *J Biomech* 2001;34:1491-1500.
14. Iberall T. Human prehension and dexterous robot hands. *Int J Robot Res* 1997;16:285-299.
15. MacKenzie CL, Iberall T. *Advances in Psychology 104: the Grasping Hand*. Amsterdam: Elsevier Science BV, 1994.
16. Cutkosky MR. On grasp choice, grasp models and the design of hands for manufacturing tasks. *IEEE Trans Robot Automat* 1989;5:269-279.
17. Rash GS, Belliappa PP, Wachowiak MP, Somia NN, Gupta A. A demonstration of the validity of a 3-D video motion analysis method for measuring finger flexion and extension. *J Biomech* 1999;32:1337-1341.
18. Darling WD, Cole KJ, Miller GF. Coordination of index finger movements. *J Biomech* 1994;27:479-491.
19. Berme N, Paul JP, Purves WK. A biomechanical analysis of the metacarpo-phalangeal joint. *J Biomech* 1977;10:409-412.
20. Asada H, Slotine JE. *Robot Analysis and Control*. New York: John Wiley and Sons, 1986.
21. Jones RD. Measurement of sensory-motor control performance capacities. Tracking tasks. In: Bronzino JD. *The Biomedical Engineering Handbook*, 2nd edn, Vol. II. Boca Raton: CRC Press, 2000.